Properties of FIR-bright ADF-S galaxies

K. Małek[1,2], A. Pollo[2,3], T. T. Takeuchi[1], V. Buat[4],
D. Burgarella[4], E. Giovannoli[4,5], M. Malkan[6]

[1] Department of Particle and Astrophysical Science, Nagoya University, Furo-cho, Chikusa-ku, 464-8602 Nagoya, JAPAN; JSPS Fellow (P11802)
[2] National Centre for Nuclear Research, ul. Hoża 69, 00-681 Warszawa, POLAND
[3] The Astronomical Observatory of the Jagiellonian University, ul. Orla 171, 30-244 Kraków, POLAND
[4] Laboratoire d'Astrophysique de Marseille, OAMP, Universite Aix-Marseille, CNRS, 38 rue Frerdeic Joliot-Curie, 13388 Marseille, cedex 13, FRANCE
[5] University of the Western Cape, Private Bag X17, 7535, Bellville, Cape Town, SOUTH AFRICA
[6] Department of Physics and Astronomy, University of California, Los Angeles, CA 90024, USA

We present the results of the analysis of multiwavelength Spectral Energy Distributions (SEDs) of far-infrared galaxies detected in the AKARI Deep Field-South (ADF-S) Survey.

AKARI ADF-S survey

The primary purpose of the IR Japanese AKARI satellite mission was to obtain a catalogue with better spatial resolution and wider spectral coverage than IRAS. To improve the knowledge of IR astrophysical sources, AKARI provided deeper observations of two fields centered on the North (NEP) and South (ADF-S) Ecliptic Poles. The ADF-S was selected for observations because it can provide the highest quality FIR extragalactic image of the Universe. This survey is unique in having continuous wavelength coverage with four photometric bands (65, 90, 140, and 160μm) mapped over a wide area (12 sq^2). To 20 mJy at 90μm 2268 infrared sources were detected, and IR colours for about 400 of these were measured.

SAMPLE SELECTION

► AKARI ADF-S catalog presented by Małek et al. 2010* + additional measurements, mostly from WISE and GALEX, and spectro-z (Sedgwick et al., 2010).
► galaxies with at least six photometric measurements in the whole spectral range from UV to FIR (95 galaxies with, and 127 without known spectro-z).

PHOTOMETRIC REDHIFTS

We used two codes:
► **Le Phare** (Arnouts et al., 1999) – standard photo-z code based on a χ^2 fitting method between the theoretical and observed photometric catalog.
► **CIGALE** (Noll et al. 2009) - SEDs fitting code. However, since it uses a large number of models covering λ from FUV to FIR, it may be expected to provide a better photo-z for ADF-S FIR-selected sample than the standard software.

We have found that for our sample CIGALE works better with our sample then Le Phare. The possible reasons are:

► the limited number of FIR templates used by Le Phare,
► spectral coverage, in particular a small amount of optical and MIR measurements,
► spectroscopic range (z<0.25) ,
► spectral types of galaxies which dominate in our sample: photo-z of actively star forming galaxies are less reliable then the elliptical.

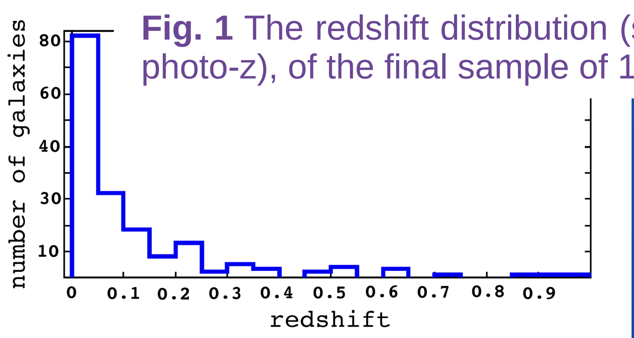

Fig. 1 The redshift distribution (spectro-z and photo-z), of the final sample of 186 galaxies

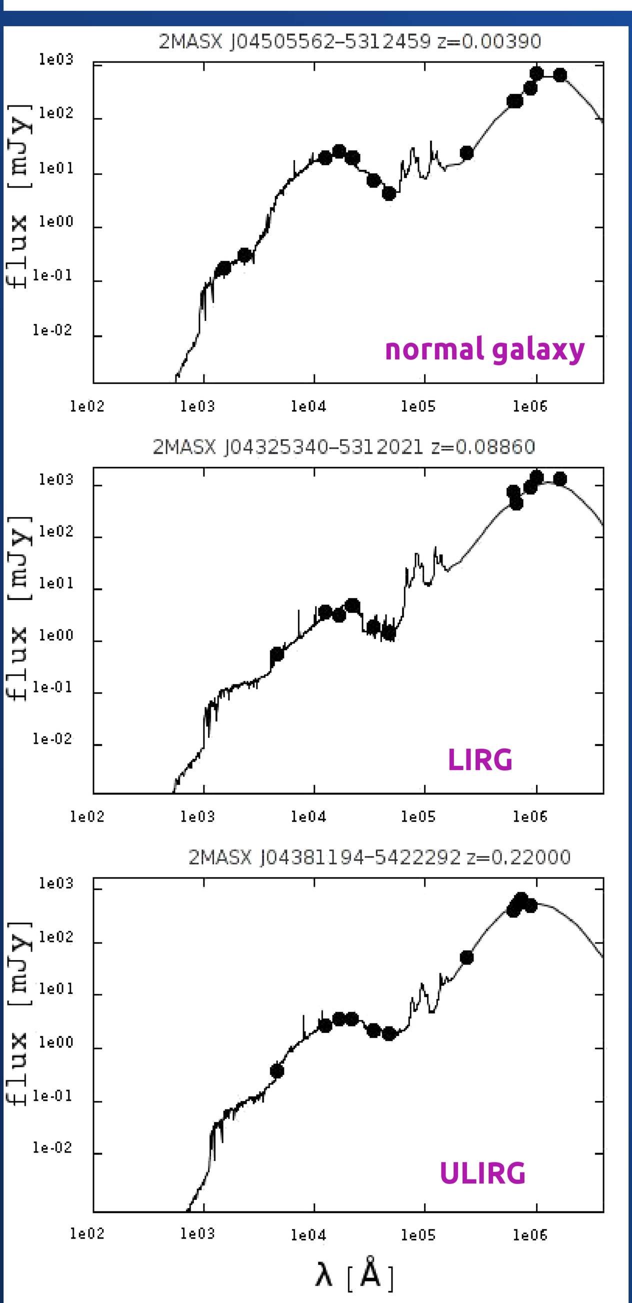

Fig. 2 Three examples of the best-fit models for the normal galaxy (upper panel), LIRG (middle panel) and ULIRG (bottom panel) sources. Solid lines correspond to the best model obtained from CIGALE code, and the full black circles - observed data used for SED fitting.

SED FITTING

CIGALE SED fitting code (Noll et al. 2009) was used to study physical parameters of the ADF-S sources. This code uses models describing the emission from a galaxy in the λ range from FUV to FIR.

In our work we have used modes:
► stellar emission - Maraston (2005),
► attenuation curves – Calzetti et al. (2000)
► dust emission – Dale & Helou (2002) + box model for the young stellar population history.

RESULTS

AVERAGE SEDs

► we created average SEDs, normalized all SEDs at rest frame 90μm;
► we divided them into: ULIRGs (9.7% of our sample), LIRGs (16.1% of our sample), and the remaining galaxies.

We noticed a significant shift in the peak λ of the dust emission in the FIR and a different ratio between luminosities in the optical and IR parts of the spectra (Małek et al., 2014). Main physical parameter obtain from CIGALE fitting are shown in Tab. 1.

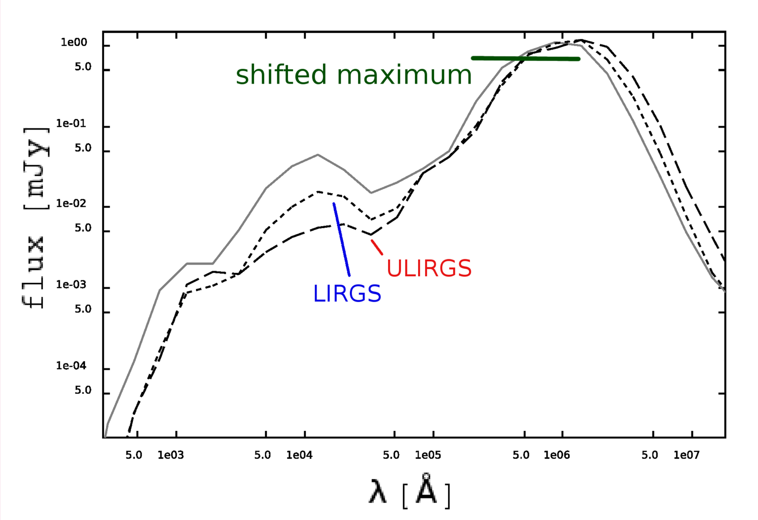

Fig. 3 The average SEDs, normalized at 90μm. SEDs were shifted to the rest frame.

	ULIRGs	LIRGs	$L_{TIR} < 10^{11} L_{\odot}$
z	0.55±0.21	0.20±0.06	0.05±0.03
$z\lambda_{max}$ [10^6 Å]	1.49±0.56	1.25±0.63	0.93±0.35
L_{bol}/L_{TIR}	0.73±0.16	0.55±0.16	0.39±0.22
logSSFR [yr^{-1}]	-9.00±0.55	-9.68±0.59	-10.28±0.57

Tab. 1 The main physical parameters (mean redshift, the λ for the max. value of dust distribution, ratio between bolometric and IR luminosity, and the Specific Star Formation Rate) for ULIRGs, LIRGs and normal galaxies from ADFS sample.

SFR vs stellar mass

► redshift distribution: mean *z* of (U)LIRG sample = 0.34 (min. and max. *z* are equal to 0.09 and 0.98, respectively)

We compared our results with:
► Elbaz et al., 2007 (*z*=0 and *z*=1),
► Daddi, et al., 2007 (*z*=2),
► with a sample of nearby (*z*<0.032) (U)LIRGs (U et al., 2012), and a sample of LIRGs observed in the GOALS survey by GALEX and SST (Howell et al., 2010)
We found a rather flat distribution of SFR parameter in the stellar mass space

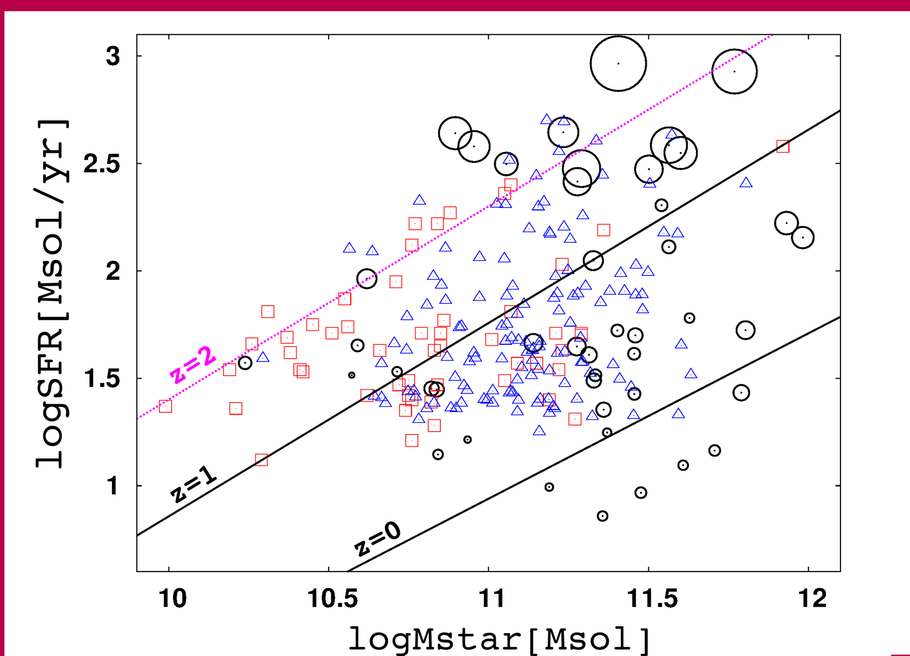

Fig. 4 The SFR vs stellar mass relation for ADF-S (U)LIRG sample (black circles). The variable size of points represents the difference in redshift (increasing size from *z* equal to 0.09 to 0.98). We overplot the Howell et al., 2010 (open blue triangles), and U et al. 2012 (U)LIRG sample (red open squares). The two solid black lines correspond to SFR vs stellar mass observation from Elbaz et al. (2007). The violet dashed line indicates the SFR - stellar mass relation for star-forming galaxies at *z*~2 defined by Daddi et al. (2007)

SSFR vs stellar mass [spectro-z only]

We compared our results with:
► Brinchmann et al. 2004 - sample of ~10^5 galaxies with measurable star formation in the SDSS in the redshift range from 0.005 to 0.220, and
► Buat et al. 2007 - nearby galaxies selected in FIR and FUV.

They found that SSRF decreases with increasing stellar mass both for FIR and UV-selected sample. Similar trend appears in ADF-S sample, however the SSFR is higher than results previously obtained (for logMstar~10, possible caused by small statistics in this range of stellar mass)

Fig. 5 Relation between the SSFR and stellar mass. The black solid line represents the volume-weighted average values of SSFR as a function of stellar mass for our sample of 73 galaxies with known spectro-z. Error bars correspond to the volume-weighted standard deviation. The stellar mass intervals are [9.9-10.3], [10.3-10.7], [10.7-11.1], [11.1-11.5].

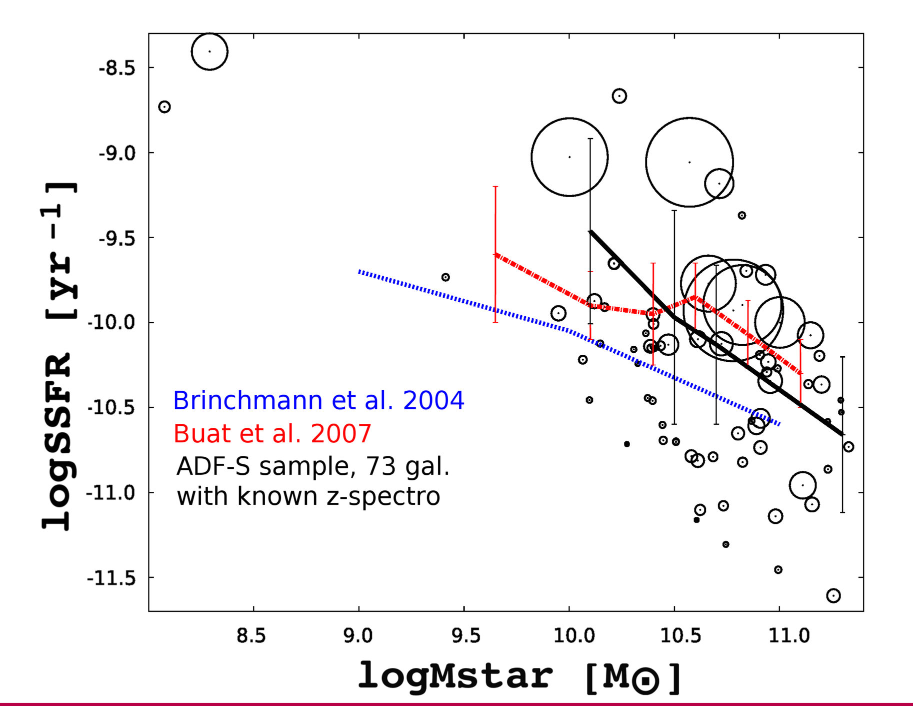

The radius of the circle is related to the flux detected at 90μm AKARI band. The distribution of fluxes shows that the lower boundary of the stellar mass vs SSFR relation corresponds to AKARI detection limit.

References:

Arnouts, S., Cristiani, S., Moscardini, L., et al., MNRAS, 310, pp. 540--556, 1999
Brinchmann, J., Charlot, S., White, S. D. M et al., MNRAS, 351, pp. 1151-1179, 2004
Buat, V., Takeuchi, T. T., Iglesias-Páramo, J., et al., ApJ, 173, pp. 404-414, 2007
Daddi, E., Dickinson, M., Morrison, G., et al., ApJ, 670, 1, pp. 156-172, 2007
Elbaz, D., Daddi, E., Le Borgne, D., et al., A&A, 468, 1, pp. 33-48, 2007
Howell, J. H., Armus, L., Mazzarella, J. M. et al., ApJ, 715, pp. 572-588, 2010
Małek, K., Pollo, A., Takeuchi, T. T., et al., A&A, 514, 511+, 2010
Małek, K., Pollo, A., Takeuchi, T. T., et al., A&A, 562, id.A15, 2014
Noll, S., Burgarella, D., Giovannoli, E., et al., A&A, 507, 1793–1813, 2009
Sedgwick, C., Serjeant, S., Pearson, C., et al., MNRAS, 416, 1862–1870, 2011
U, V., Sanders, D. B., Mazzarella, J.Met al., , ApJ Supplement, 203, 1, 2012

* The sample consists of the 545 ADF-S sources from the so-called 6σ catalog ($S_{90μm}$>0.0301Jy, which corresponds to the 6σ detection level) measured by the AKARI FIS detector, for which the optical counterparts were found in public catalogues SIMBAD, NED, and IRSA. The search for counterparts was performed within the radius of 40'' around each source.